Macromolecules
ARTICLE

Macromolecules **2009**, *42*, 8809–8816 **8809**
DOI: 10.1021/ma901801s

Functionalized Conjugated Microporous Polymers

Robert Dawson, Andrea Laybourn, Rob Clowes, Yaroslav Z. Khimyak, Dave J. Adams, and Andrew I. Cooper*

Department of Chemistry and Centre for Materials Discovery, University of Liverpool, Crown Street, Liverpool L69 7ZD, United Kingdom

Received August 11, 2009; Revised Manuscript Received October 1, 2009

ABSTRACT: A range of conjugated microporous polymer networks has been prepared using Sonogashira–Hagihara cross-coupling of 1,3,5-triethynylbenzene with a number of functionalized dibromobenzenes. Porous poly(arylene ethynylene) networks with surface areas up to 900 m^2/g were produced. The surface chemistry of the networks was varied by monomer selection, thus allowing control over physical properties such as hydrophobicity. Additionally, it was shown that the dye sorption behavior of the networks can be controlled by varying the hydrophobicity. This expands significantly on the utility of this approach, allowing high surface area networks to be prepared with properties that can be tailored for applications such as catalysis and separations.

Introduction

The design and synthesis of microporous organic polymer networks has attracted significant interest due to potential applications in areas such as molecular separations,[1] heterogeneous catalysis,[2−4] and gas storage.[1−4] Several different classes of porous organic networks have been prepared. Covalent organic frameworks (COFs)[5−8] have the highest known surface areas reported for purely organic networks (up to 4210 m^2/g).[6] These materials have good thermal stability but may be relatively moisture-sensitive.[9] Triazine networks[10−12] and hyper-cross-linked polymers (HCPs)[12,13] have apparent Brunauer−Emmett−Teller (BET) surface areas (S_{BET}) in the ranges of 584−2475 and 330−2090 m^2/g, respectively, but their synthesis requires the use of harsh conditions. In the case of triazines, ionothermal reaction conditions at > 400 °C in the presence of $ZnCl_2$ are employed[10,12] while the synthesis of HCPs involves the use of strong Lewis acids such as $FeCl_3$ and the subsequent generation of hydrochloric acid. In both cases, these harsh reaction conditions may preclude the incorporation of certain chemical functionalities. Polymers of intrinsic microporosity (PIMs)[15−18] utilize monomers with rigid, twisted structures to produce materials with surface areas ranging from 500 to 750 m^2/g in the case of linear polymers and up to 1064 m^2/g in the case of PIM networks.[19] Uniquely, linear PIMs are soluble and can be cast from solution as porous films with good mechanical properties.

There has been recent interest in the synthesis of conjugated microporous polymers (CMPs) via palladium cross-coupling of di- or trihalo aromatics with di- or triethynyl aromatics to produce porous poly(arylene ethynylene)s (PAEs).[20−23] We have shown that the pore sizes for such PAE networks can be fine-tuned by changing the strut length of the monomers, thus increasing or decreasing the pore volume and surface area of the products.[21] It was also shown that smaller strut lengths in the monomers lead to an increase in the surface area of the resulting polymers.[21] Surface areas of up to 1213 m^2/g could be achieved by utilizing a tetrahedral monomer.[22] Other related work has shown that microporous poly(arylene thienylene)s can be prepared by Suzuki coupling,[3] while Kaskel and co-workers have synthesized microporous hydrophobic polysilanes (S_{BET} up to 1046 m^2/g) via an organolithiation route.[24] Kobayashi and co-workers have described the indirect preparation of porous pyrolytic polymers via treatment of alkyl-substituted poly(phenylenevinylene) precursors at high temperatures (> 350 °C).[25,26] Recently, the synthesis of microporous crystalline networks using Schiff base chemistry was reported[27,28] with crystalline materials showing high surface areas of 1360 m^2/g[28] and an amorphous network exhibiting a somewhat lower surface area of 750 m^2/g.[27]

CMP networks prepared so far by Pd cross-coupling chemistry have involved a relatively narrow range of monomers. In addition to our first reports,[20−22] there are examples of the use of triphenylamine monomers,[29] thienyl monomers,[3] and silicon-centered, tetrahedral monomers.[22] There have been few examples however of using diversity in monomer structure as a means to modify physical properties other than surface area. By contrast, metal−organic frameworks (MOFs) can combine tunable porosity with a range of different organic functionalities.[30] For example, it was shown that higher heats of adsorption for H_2 were obtained at low gas coverage when the pores in the MOF were modified with methyl groups.[30] This was achieved, however, at the cost of overall pore volume and therefore total H_2 storage capacity. A naphthalene-based MOF was shown to have a good combination of high heats of adsorption for H_2 while maintaining a high overall uptake.[30] The development of microporous polymer networks which incorporate a range of different chemical functionalities should allow us to access functional materials for a wider range of applications, beyond the "tuning" of enthalpies of sorption for gases. For example, the ability to fine-tune functionality might enhance the selectivity of molecular separations or catalytic processes. It is therefore desirable to investigate methods to incorporate a wide variety of functionality into porous organic networks. We describe here a series of PAE networks synthesized by direct ($A_3 + B_2$) palladium-catalyzed cross-coupling polycondensation incorporating a broad range of chemical functionalities in the B_2 monomer.

Experimental Section

Materials. 1,3,5-Triethynylbenzene was obtained from ABCR and used as received. All other chemicals and solvents were obtained from Sigma-Aldrich and used as received. Anhydrous

*Corresponding author. E-mail: aicooper@liverpool.ac.uk.

Published on Web 10/29/2009

Scheme 1. Synthetic Route to Networks 1−22[a]

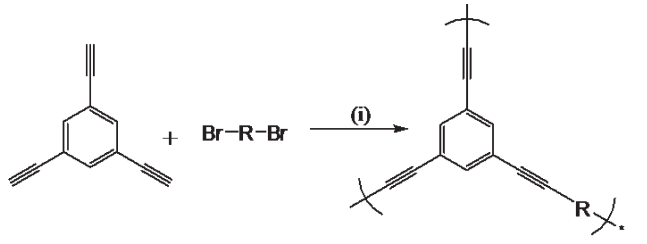

Where Monomer B is one of the following dibromo monomers:

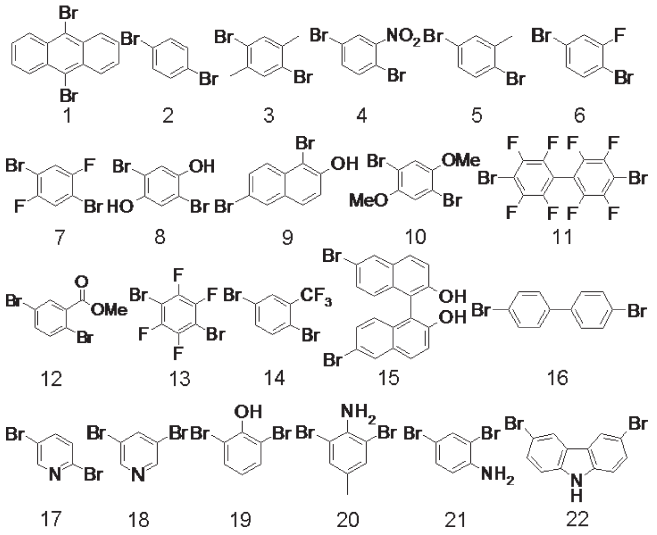

[a] Conditions: (i) toluene:Et_3N (1:1), $Pd(PPh_3)_4$, CuI, 80 °C, 72 h.

grade toluene and triethylamine were used throughout (Sigma-Aldrich). All chemicals used had a purity of 97% or greater.

Synthesis of PAE Networks. All of the networks were synthesized by palladium-catalyzed Sonogashira−Hagihara cross-coupling condensation reaction of arylethynylenes and arylhalides.[20−22] In a typical procedure, 1,3,5-triethynylbenzene (1 mmol) and dibromomonomer (1 mmol) were placed in a Radley's 6-place carousel 100 mL round-bottom flask which was degassed and backfilled with nitrogen gas. A 1.5 M excess of ethynyl groups was used as previously described.[20] The solids were dissolved in a mixture of anhydrous toluene (1.5 mL) and anhydrous triethylamine (1.5 mL) and heated to 50 °C. When the solution had reached this temperature, a slurry of tetrakis-(triphenylphosphine)palladium(0) (50 mg, 0.04 mmol) and copper(I) iodide (15 mg, 0.08 mmol) in anhydrous toluene (1 mL) was added, the temperature raised to 80 °C, and the reaction stirred under nitrogen for 3 days. The solid product was then collected by filtration and washed well with toluene and methanol before being Soxhlet extracted with methanol for 16 h. The products were dried in vacuo at 60 °C for 16 h to give insoluble light to dark brown solids. Example data for network **2** (see Scheme 1). Average yield: 250 mg (112%). FTIR: 3303 (−C≡C−H), 3056 ($-C_{Ar}-H$) 2208 (−C≡C−), 1582 ($-C_{Ar}=C_{Ar}-$). Analysis: Calculated for network **2**: C, 96.55; H, 3.45. Found: C, 79.02; H, 3.64. The higher than expected yield and deviation of the elemental analysis from theory can be accounted for by the unreacted alkyne and bromophenyl end groups identified by solid-state NMR as well as (to a lesser degree) catalyst residues identified by EDX.

Gas Sorption Analysis. Polymer surface areas and pore size distributions were measured by nitrogen adsorption and desorption at 77.3 K using either a Micromeritics ASAP 2420 or ASAP 2020 volumetric adsorption analyzer. The surface areas were calculated in the relative pressure (P/P_0) range from 0.01 to 0.05 (see Supporting Information). Pore size distributions and pore volumes were derived from the adsorption branches of the isotherms using the nonlocal density functional theory (NL-DFT) pore model for pillared clay with cylindrical pore geometry. Samples were degassed at 120 °C for 15 h under vacuum (10^{-5} bar) before analysis. Hydrogen isotherms were measured at 77.3 and 87.3 K up to 1.13 bar using a Micromeritics ASAP 2420 volumetric adsorption analyzer.

Infrared Spectroscopy. IR spectra were collected in reflectance using a Bruker Tensor 27 fitted with HT-XTS cooled with liquid N_2.

Scanning Electron Microscopy. High-resolution imaging of the polymer morphology was achieved using a Hitachi S-4800 cold field emission scanning electron microscope (FE-SEM). The dry samples were prepared on 15 mm Hitachi M4 aluminum stubs using either silver dag or an adhesive high-purity carbon tab. The samples were then coated with a 2 nm layer of gold using an Emitech K550X automated sputter coater. The FE-SEM measurement scale bar was calibrated using certified SIRA calibration standards. Imaging was conducted at a working distance of 8 mm and a working voltage of 3 kV using a mix of upper and lower secondary electron detectors.

Solid-State NMR. Solid-state NMR spectra were measured on a Bruker Avance 400 DSX spectrometer operating at 100.61 MHz for ^{13}C and 400.13 MHz for ^{1}H. $^{1}H-^{13}C$ cross-polarization magic angle spinning (CP/MAS) NMR experiments were carried out at an MAS rate of 10.0 kHz using zirconia rotors 4 mm in diameter. The ^{1}H $\pi/2$ pulse was 3.0 μs, and two-pulse phase modulation (TPPM) decoupling[31] was used during the acquisition. The Hartmann−Hahn condition was set using hexamethylbenzene. The spectra were measured using a contact time of 2.0 ms and a relaxation delay of 8.0 s. Typically, 2048 scans were accumulated. The values of the chemical shifts are referred to that of TMS. The analysis of the spectra (deconvolution and integration) was carried out using Bruker TOPSPIN software.

Thermogravimetric Analysis (TGA). TGA analysis was carried out using a Q5000IR analyzer (TA Instruments) with an automated vertical overhead thermobalance. The samples were heated at the rate of 5 °C/min under a nitrogen atmosphere.

Contact Angle Measurements. 40 mg of polymer powder was pressed into a disk using 10 tons of pressure. 10 μL of water was placed onto the surface of the disk. Photographs were taken of this droplet and the contact angle measured.

Methyl Orange Uptake. Aqueous solutions of methyl orange were prepared a number of concentrations (from 25 to 1000 g/m^3). 10 mL of a solution at a known concentration were added to 20 mg of polymer. The mixture was shaken for 24 h at 25 °C, after which the solution was diluted, and the maximum absorption was measured at 465 nm on a Powerwave UV−vis spectrometer and compared to a calibration curve made without the addition of polymer.

Results and Discussion

We have demonstrated previously that Sonogashira−Hagihara palladium-catalyzed cross-coupling can be used to prepare PAE networks which are highly microporous.[20−22,29] In general, we have utilized diiodo-B_2 monomers in an $A_3 + B_2$ polycondensations to prepare these networks.[20−22,29] There are however relatively few commercially available diiodo-monomers. As such, we focus here on the use of dibromo monomers for the introduction of functionality. Brominated molecules are known to react more slowly in Sonogashira cross-coupling reactions than the iodo equivalents.[32] A modified synthetic procedure was used for the reaction of dibromo monomers with 1,3,5-triethynylbenzene (Scheme 1). The best reproducibility in terms of surface area and yield was achieved by addition of the catalyst as a slurry to the monomer solution at 50 °C before then elevating the temperature to 80 °C for the remainder of the reaction.

A range of dibromo-monomers was chosen to incorporate different chemical functionality into the networks. Functionalities included hydrophobic and hydrophilic groups, potentially chelating pyridyl groups, and monomers with electron-donating or electron-withdrawing groups functionality (Scheme 1). The polycondensation was found to be tolerant to a broad range of functionality, including methyl, fluoro, amino, nitro, trifluoromethyl, hydroxy, methoxy, and pyridyl groups. The presence of electron-withdrawing groups is also known to increase reactivity in Sonogashira coupling reactions.[33] Hence, the different functional groups in these monomers might also be expected to have a significant effect on the degree of condensation. Two of these monomers, **2** and **16**, are simply the brominated analogues of the monomers used by us previously to prepare "nonfunctionalized" PAE networks.[20,21] In addition to 1,4-dibromo-substituted monomers, we also explored monomers which were meta-substituted (**18**−**22**) as well as some larger polyaromatic monomers (**1**, **9**, **11**, **15**, **16**, and **22**). As found for PAE networks prepared from diiodo monomers,[20] all networks precipitated from solution as brown powders that were found to be insoluble in all solvents tested. Qualitatively, we observe that precipitation of the network from solution takes significantly longer for the less reactive brominated monomers used here compared to equivalent iodo monomers described previously. After reaction, the networks were collected by filtration and washed exhaustively via Soxhlet extraction to remove any residual monomer and catalyst residues.

The polymers were characterized at the molecular level by $^{1}H-^{13}C$ CP/MAS NMR in order to confirm the inclusion of the different functional groups in the polymer networks, particularly since it is possible in principle to form porous homocoupled polybutadiynylene networks from alkyne−alkyne reactions in cases where the bromo-functionalized monomers are insufficiently reactive.[34] Examples of the NMR spectra are shown in the Figure 1, and assignment of the peaks is given in Table 1. All networks show aromatic peaks at ca. 134 ppm (C_{Ar-H}) and 124 ppm ($C_{Ar}-C\equiv C-C_{Ar}$), consistent with CMP networks synthesized previously.[20,21] The NMR spectrum for network **2** (the analogue of the previously described CMP-1) was similar to that reported for the network prepared from the iodated monomer.[20,21] However, the degree of condensation for the two networks was found to be different. The ratio of alkyne to aromatic peaks is calculated to be 0.40 if one assumes complete condensation of alkyne groups and ideal stoichiometry in the resulting polymeric structures. By experiment, the iodinated CMP-1 network had an alkyne to aromatic peak ratio of 0.27[20,21] while the analogous brominated network **2** had a corresponding ratio of 0.16. Coupled with the lower ratio of terminal alkyne:quaternary alkyne peak intensity that was observed (Table 1), this implies a greater number of aromatic end groups for **2** and hence a lower degree of polycondensation. Both **2** and CMP-1 showed a broad shoulder at ca. 137 ppm, which may originate from H-bearing carbons in aromatic end groups that bear residual halogen groups.[20,21] A lower than predicted degree of condensation was also implied by the high yields and the elemental analyses observed for **2**. Indeed, EDX analysis of **2** showed 3.64 wt % bromine in the network compared with 2.27 wt % iodine estimated for CMP-1.[20,21] Elemental analysis for network **2** also demonstrated carbon and hydrogen contents that were lower than observed for CMP-1 (carbon, 79.02%; hydrogen, 3.64% as compared to carbon, 86.37%; hydrogen, 4.75% for CMP-1).[20,21] For network **16**, a direct analogue of the previously reported CMP-2,[20,21] from the NMR data, it is clear that there almost no terminal alkyne present in this network. The intensities in the aromatic region are significantly different to that previously reported for CMP-2 prepared from the iodinated monomer. Again, this can be ascribed to the lower reactivity of the brominated monomer used in this study and hence a lower degree of condensation.

The NMR spectra for the networks (Figure 1) also proved that cross-coupling had occurred and that the products were not simply the result of homocoupling of the 1,3,5-triethynylbezene monomer.[34] Resonances assigned to C_{Ar-Br} end groups in the networks were observed as a shoulder on the main aromatic peaks at 136−138 ppm. The relative concentration of alkyne end groups (83 ppm) as compared to total alkyne functionality present was elucidated by spectral deconvolution in the alkyne region (see Supporting Information for example deconvolution data, Figures S6.1 to S6.2). From this data (Table 1), it was clear that the more electron-withdrawing fluorinated networks in particular contained a substantial fraction of terminal alkyne end groups. By contrast, network **2** was found to have the lowest percentage of alkyne end groups. From these data, it seems clear that the end groups are mainly halogens for network **2**, but alkynes for the networks prepared from more electron-withdrawing monomers such as **7** and **14**. This is in agreement with the generally observed trend of greater reactivity for monomers bearing electron-withdrawing groups.[32] However, network **4** shows a similar low level of alkyne end groups to network **2** despite the presence of the highly electron-withdrawing nitro group. This indicates that the electronic effect of the dibromo monomer does not always lead to similar levels of condensation. The amine-functionalized networks (**20** and **22**) both show low values for the ratio of alkyne end groups to total alkyne (0.18 and 0.07), respectively, demonstrating that efficient coupling occurred in these systems.

The pore structures of these PAE networks were investigated by gas sorption analysis using N_2 and H_2 as sorbates. The BET surface area, S_{BET}, of the network **2** compared well with that reported for the iodinated CMP-1 analogue (entry **2**: 867 m^2/g; CMP-1: 834 m^2/g[20]). In the majority of cases, the Sonogashira−Hagihara cross-coupling reaction led to PAE networks with significant porosity (Table 2). Interestingly, many of the monomers, such as those containing methyl, fluoro, and hydroxyl groups, produced materials with a surface area that was very similar to the parent network, **2**. Some networks were found to have relatively low BET surface areas. These include the network formed by reaction of 6,6′-dibromo-1,1′-binaphthol with 1,3,5-triethynylbenzene (**15**), which produced an insoluble nonporous material. It is clear from entry **8** that this reaction is tolerant of hydroxyl functionality since the reaction of 2,5-dibromohydroquinone resulted in a porous network. We therefore tentatively ascribe the lack of porosity in the case of the 6,6′-dibromo-1,1′-binaphthol to binding of the catalyst to the monomer resulting in a very low level of condensation and hence porosity. Previous Sonogashira−Hagihara coupling to a binaphthol derivative utilized the acetoxy-protected compound.[35] This may be due to the bidentate nature of the binaphthol monomer which contrasts with other monomers such as the pyridyl- and amine-containing species in networks **17**, **18**, and **20** which might also in principle bind to the catalyst but which are monodentate in nature. Thermogravimetric analysis showed that the majority of the networks formed were stable to 300 °C or greater (see Figures S4.1 to S4.22).[21] Other networks showing low S_{BET} included **16**, which is a direct analogue of CMP-2.[20,21] As noted above, we ascribe the lower surface area to the relatively low reactivity of brominated monomers as compared to the iodinated analogues.

Initial screening of the porosity in the networks was carried out by collecting five points of the N_2 isotherm in the relative pressure range 0.05−0.3. This demonstrated that of the 22 different networks prepared 13 had surface areas over 500 m^2/g. These 13 networks were then investigated in more detail by collecting the full nitrogen and hydrogen isotherms. The highest apparent BET surface area achieved in this library was 880 m^2/g (network

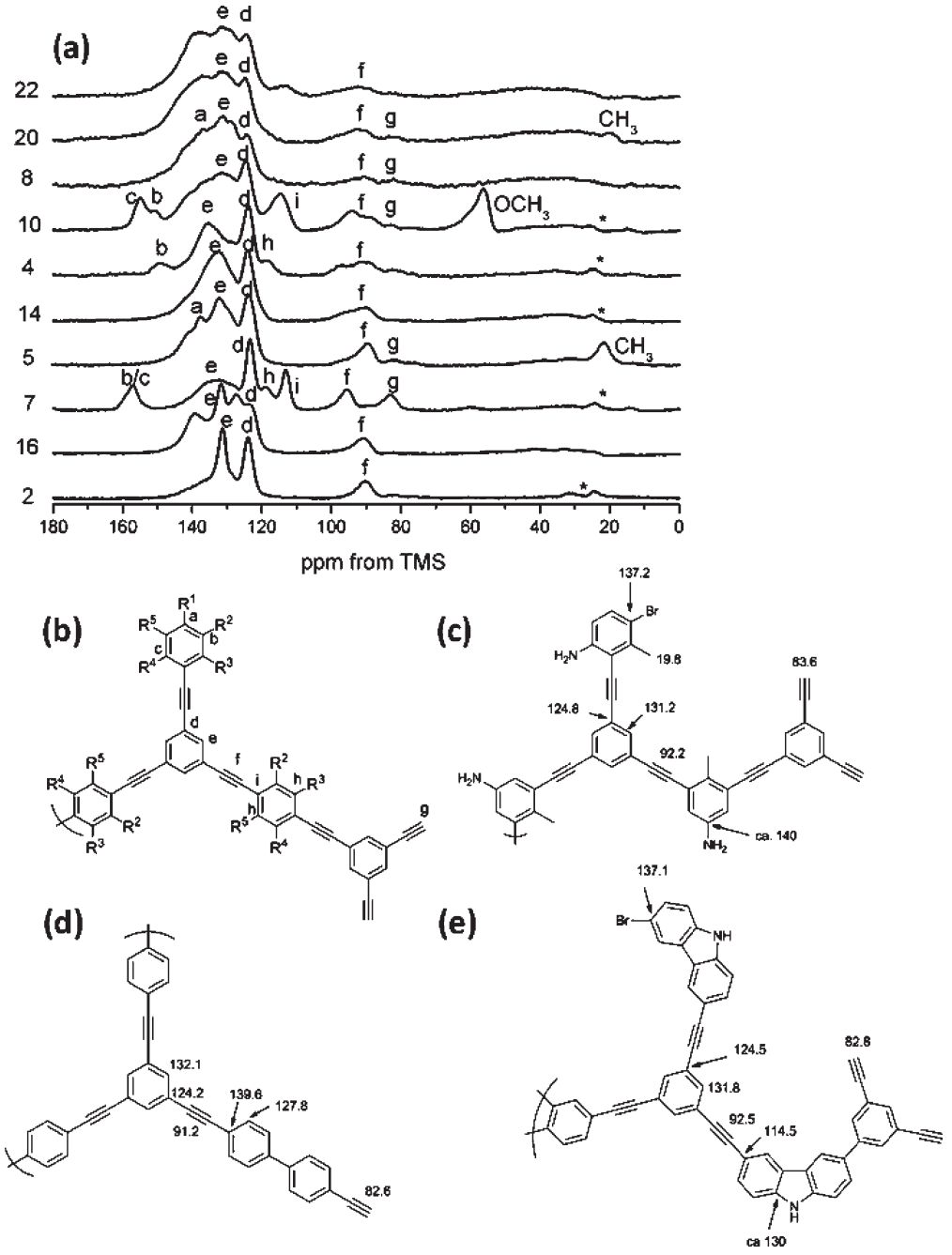

Figure 1. (a) Solid-state $^{1}H-^{13}C$ CP/MAS NMR spectra for example functionalized conjugated microporous PAE networks recorded at an MAS rate of 10 kHz. Asterisks denote spinning sidebands. (b) General structure of the repeat units for PAE networks (c) Structure and assignment for network **20**. (d) Structure and assignment for network **16**. (e) Structure and assignment for network **22**.

Table 1. Peak Assignments Corresponding to the NMR Spectra in Figure 1b (All Values in ppm)

network	a	b	c	d	e	f	g	h	i	other	ratio[a]
2				124.0	131.4	90.2					0.15
4		149.4		124.1	135.3	90.7			118.0		0.15
5	138.0			124.4	132.6	89.9	83.2			22.0 (CH_3)	0.16
7		157.5	157.5	123.8	132.5	95.9	83.1	119.2	113.5		0.80
8	136.9	≈150		124.6	131.3	90.1	82.2				0.35
10		150.8	155.1	124.8	131.6	94.1	83.0	114.8		56.4 (OCH_3)	0.08
14		≈122		124.2	132.3	90.0					0.77

[a] Ratio of integration of terminal alkyne: quaternary alkyne.

19). These values for the BET surface areas are broadly in comparable with those obtained for other networks prepared via Sonogashira−Hagihara coupling.[20−23,29] The networks gave rise to either type I or IV N_2 gas sorption isotherms according to IUPAC classifications,[36] indicating the presence of both micropores and mesopores/small macropores, most likely arising from interparticulate porosity. Micropore volumes of between 0.20 and 0.33 cm^3/g were calculated from the total pore volume at

$P/P_0 = 0.1$, indicating significant microporosity and comparable to that observed for CMP-1 (0.33 cm^3/g).[20,21] Total pore volumes of up to 1.78 cm^3/g were achieved, and this can be explained by the relatively large population of larger pores indicated by the type IV isotherms. Example data for a subset of the networks are shown in Figure 2, with data for all materials available in the Supporting Information (Figures S1.1.1 to S1.1.13) The isotherms found for this library of materials differed from the previously reported PAE networks prepared from diiodo-monomers which all exhibited more classical type I isotherms.[20,21]

Table 2. A Series of Networks Prepared by Sonogashira−Hagihara Coupling

network	S_{BET} (m^2/g)	S_{Lang} (m^2/g)	$V_{0.1}$ (cm^3/g)[c]	V_{Tot} (cm^3/g)[d]	$V_{0.1}/V_{Tot}$	wt % H_2
1	136[a]					
2	867[b]	1046	0.33	0.99	0.33	1.08
3	682[b]	912	0.25	1.06	0.24	0.81
4	247[a]					
5	739[b]	964	0.27	1.50	0.18	0.91
6	723[b]	896	0.27	0.87	0.31	0.85
7	690[b]	842	0.27	0.52	0.52	0.86
8	761[b]	1026	0.27	1.73	0.16	0.90
9	648[b]	796	0.26	0.55	0.47	0.92
10	293[a]					
11	140[a]					
12	322[a]					
13	853[b]	1077	0.32	0.94	0.34	1.14
14	803[b]	1002	0.31	0.47	0.70	0.86
15	3[a]					
16	204[a]					
17	42[a]					
18	262[a]					
19	880[b]	1155	0.33	1.78	0.19	0.90
20	542[b]	721	0.20	0.97	0.21	0.77
21	637[b]	834	0.24	1.07	0.22	0.74
22	779[b]	1011	0.29	1.40	0.21	0.92

[a] Based on 5-point BET pressure range 0.05−0.3 P/P_0. [b] Based on full isotherm pressure range 0.01−0.05 P/P_0. [c] Pore volume at $P/P_0 = 0.10$. [d] Total pore volume at $P/P_0 = 0.99$. Langmuir surface areas, pore volumes, and hydrogen uptakes were only collected for networks containing significant microporosity (i.e., those with a $SA_{BET} > 500$ m^2/g).

Several of the isotherms resemble those reported for polymers resulting from the polymerization of tetrakis(4-bromophenyl)silane with di- and triethynylbenzene,[22] where we observed pronounced pore filling at higher relative pressures as well as some hysteresis upon desorption. In contrast, polymerization of the carbon-centered tetraiodo analogue gave rise to a straight type I gas sorption isotherm.[22] We ascribed this difference to phase separation that occurred during the synthesis, rather than any molecular structural difference between the silicon- and carbon-centered polymers.[22] We also note that type IV isotherms were also observed for the network prepared using a 3-dimensional brominated spiro-monomer reported by Weber et al.[23] In all of these cases,[22,23] a common factor is the use of brominated rather than iodinated monomers. It is likely that this lower reactivity influences the degree of condensation in the networks and that this (and possibly the very different reaction kinetics) influences the phase behavior and hence the degree of "nonmolecular" interparticulate porosity observed in the materials. Indeed, we note that those networks that give rise to surface areas below 500 m^2/g show the presence of larger, fused masses which are absent in those with higher surface areas (see Supporting Information). We previously observed similar structures for the polymerizations with the tetrakis(4-bromophenyl)silane monomer.[22] Some monomer combinations give rise to interparticulate porosity as described previously for cross-linked resins in the presence of a porogen[37] while others do not. This may be related to the solvation or lack of solvation by the porogenic solvent medium for the different polymer networks as a function of chemical structure, as rationalized by Sherrington.[37] To estimate the contribution of microporosity to the total porosity in the networks, we have calculated the ratio of $V_{0.1}/V_{Tot}$, the ratio of the pore volume at $P/P_0 = 0.10$ to the total pore volume at $P/P_0 = 0.99$. There is some indication that the monomers containing more electron-withdrawing groups lead to networks with higher microporosity: for example, **7** and **14** give a higher ratio of $V_{0.1}/V_{Tot}$. However, network **9** also has a relatively high $V_{0.1}/V_{Tot}$

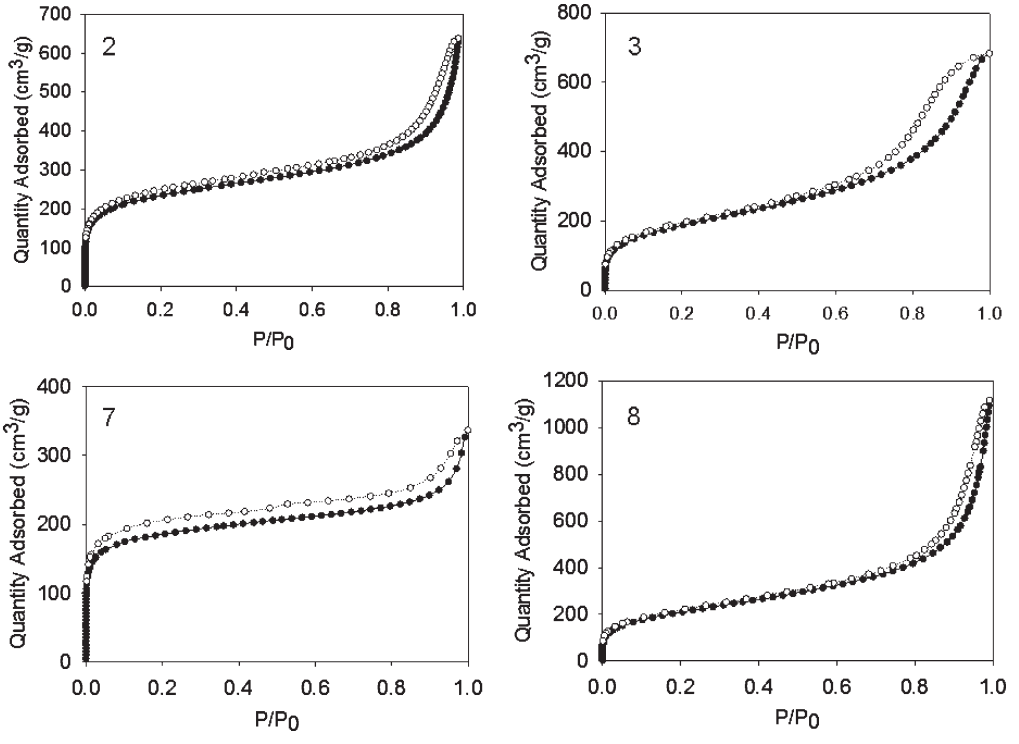

Figure 2. Example N_2 adsorption−desorption isotherms collected at 77 K for networks **2**, **3**, **7**, and **8**.

Table 3. Contact Angle Measurements As Determined from Four Repeat Measurements from Pressed Disks of the Polymer Networks

network	**2**	**5**	**3**	**6**	**7**	**13**	**8**	**19**
functional group(s)	none	CH_3	CH_3	F	F	F	OH	OH
contact angle (deg)	90 ± 12	89 ± 13	96 ± 10	103 ± 7	120 ± 22	94 ± 15	61 ± 9	68 ± 3

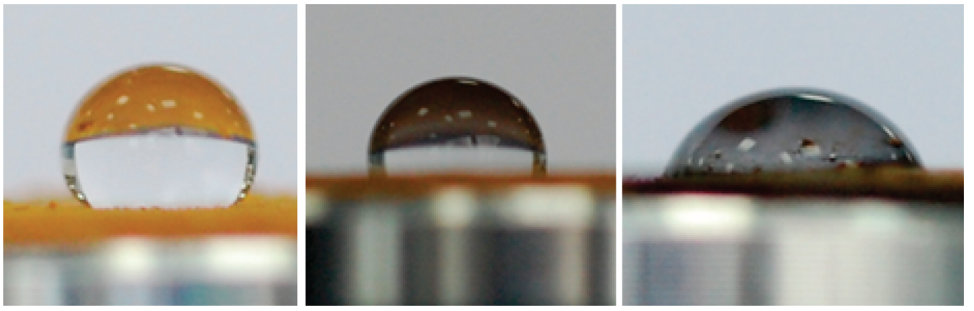

Figure 3. Contact angle images for networks (left) **7**, (middle) **2**, and (right) **3** with water.

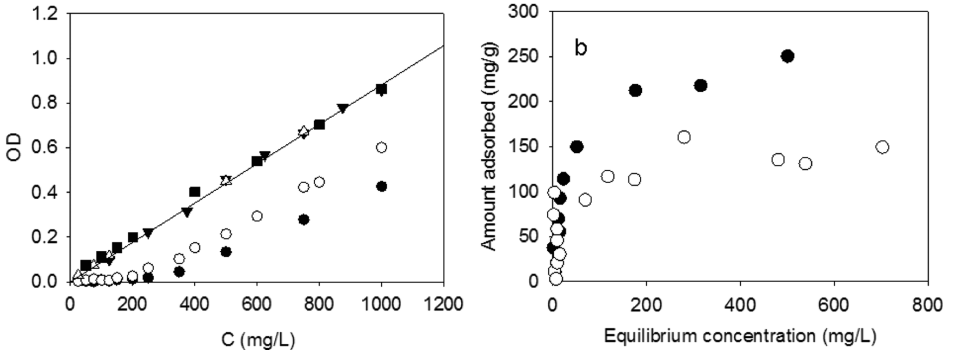

Figure 4. (a) Adsorption of methyl orange by networks **2** (△), **5** (■), **8** (○), and **19** (●) as compared to the calibration curve (no polymer present, ▼, with the line added as a guide to the eye). (b) Methyl orange adsorption isotherms for networks **8** (○) and **19** (●) derived from the data in (a).

ratio, suggesting that simple electronic effects are not the sole influence here.

The hydrogen isotherms were also measured for networks with BET surface areas greater than 500 m^2/g. Network **2** shows a H_2 uptake of 1.08 wt % at 77.3 K and 1.13 bar, similar to that found previously for CMP-1 (1.14 wt %).[21] Network **13** showed a slightly higher uptake of 1.14 wt % while other networks showed H_2 uptakes of between 0.74 and 0.92 wt %.

High surface area materials are of value in a number of applications. Many of these require specific surface properties such as hydrophobicity or polarity, in addition to the high permanent surface area.[38] The library prepared in this study contains a number of materials which have quite similar porosity but contain very different functional groups. It is therefore of interest to ascertain the influence of these functional groups on the surface properties of the networks. We have first concentrated on the hydrophobicity of the networks. To estimate the hydrophobicity of these PAE materials, we shaped various networks into disks using a high-pressure press. Contact angles with water were then measured on these surfaces (Table 3) as described elsewhere (see Figures S2.1−2.4).[39,40] The parent network, **2**, showed a contact angle with water of 90°. Networks **5** and **3**, with one and two methyl groups per B_2 monomer, respectively, showed similar contact angles (89° and 96°). The fluoro-substituted networks, **6**, **7**, and **13**, showed significantly higher contact angles than the parent network (103°, 120°, and 94°, respectively) as might be expected for networks incorporating fluorine. By contrast, the measured contact angles for the hydroxy-substituted networks **8** and **19** are much lower (61° and 68°, respectively). It is therefore clear that the hydrophobicity of the networks can be controlled by varying the hydrophobicity of the B_2 monomer. We note that in all cases the BET surface areas are similar. Some differences are observed between the pressed-disk morphologies of the different polymers. For example, the disk prepared from **19** is relatively smooth compared to the other samples. However, the disk prepared from **8**, which has a similar contact angle to **19**, is much rougher and, qualitatively, as rough as those prepared from **2** or **6** (with higher contact angles). We therefore do not believe that the surface roughness alone would account for these quite large variations in contact angle. Some morphological changes might be expected on the basis of the sorption isotherms. Networks **2** and **8** were found to have low values of $V_{0.1}/V$, implying a relatively high level of mesoporosity. Network **7** has a much higher value of $V_{0.1}/V_{Tot}$. It is possible therefore that the high contact angle also reflects this to some degree, although we note that the contact angles for **2** and **5** are very similar, whereas there is a significant difference between the values for $V_{0.1}/V_{Tot}$ for these materials.

To further probe the hydrophobicity and demonstrate molecular differences between networks, we examined dye adsorption in this subset of networks. Recent work by others has demonstrated that triazine-based networks can be used to adsorb high quantities of dye from aqueous solution.[41] Similarly, a microporous phthalocyanine network was been used as an adsorbent for a range of probe molecules.[42] This phthalocyanine network was shown to be more selective than an activated charcoal, adsorbing smaller molecules but rejecting larger molecules. For such applications, a high surface area is key in terms of maximum adsorption capacity, but it is also clear that the porous surface

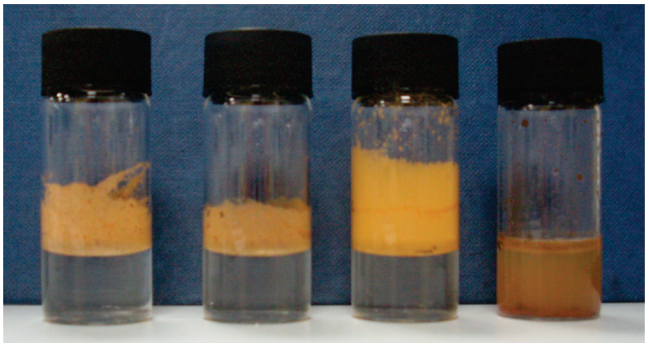

Figure 5. Photographs demonstrating the hydrophobicity of different networks. From left to right, networks **2**, **3**, **5**, **7**, and **8** (20 mg) in water (5 mL).

must be wettable for uptake to be successful. As an example of a hydrophilic dye, we used methyl orange following the work of Kuhn et al.[41] The networks were suspended in aqueous solutions of methyl orange of varying concentration and mixed well. After 3 days, samples were removed and the amount of dye adsorbed on the networks was calculated spectroscopically (see Figure 4). The different hydrophobicities of the networks result in varying behavior. The more hydrophobic networks, **2** and **5**, did not mix well with the aqueous dye solutions (Figure 5). On the other hand, the more hydrophilic network **8** was wetted efficiently by the solution (Figure 5). Unsurprisingly, no dye uptake was observed in networks **2** or **5**. However, networks **8** and **19** showed significant dye uptake. The adsorption isotherms are shown in Figure 3. The data demonstrate that **8** becomes saturated with dye at a lower concentration than **19** despite the close match in BET surface area (Table 2). Both networks adsorb less dye than the carbonaceous polymers described previously[41] which had higher surface areas than the networks used here as well as greater mesoporous character. Again, we note that networks **5**, **8**, and **19** have similar values for $V_{0.1}/V_{Tot}$ (Table 2), but only the more hydrophilic networks, **8** and **19**, adsorb dye. This indicates the importance of the monomer choice as opposed to simply the porosity of the networks.

Conclusions

We have demonstrated that porous PAE networks can be synthesized with a range of functionalities and with moderate to high surface areas using the Sonogshira−Hagihara cross-coupling reaction of functionalized dibromobenzenes with 1,3,5-triethynylbenzene. This polymerization was found to be tolerant to a wide range of functionality, including methyl, fluoro, amino, nitro, trifluoromethyl, hydroxy, methoxy, and pyridyl groups. The resulting networks have been characterized by solid-state NMR, and the data imply a lower degree of polycondensation in comparison with equivalent networks prepared from iodinated monomers. The resulting networks show type IV or type I gas sorption isotherms, and apparent BET surface areas of up to 880 m^2/g have been obtained. These networks exhibit quite different hydrophobicities depending on the functionality of the B_2 monomer, as demonstrated by contact angle measurements. Networks incorporating hydroxyl groups are efficiently wetted by water and can be used to adsorb methyl orange from aqueous solution. The more hydrophobic networks do not wet effectively with water and hence do not adsorb dye from aqueous solutions. We have thus shown that the surface properties of amorphous polymer networks can be tuned by monomer choice. This expands significantly on the utility of this approach, and future studies will concentrate on the influence of linker functionality on gas sorption properties, in particular on the isosteric heat of sorption with gases such as methane.[43]

Acknowledgment. We thank the EPSRC (EP/C511794/1) for funding. We thank Tom Hasell for running the EDX experiments. A.I.C. is a Royal Society Wolfson Merit Award holder.

Supporting Information Available: Full gas sorption isotherms for all networks, TEM for all networks, further information on the contact angle measurements, and example deconvolution of the NMR data. This material is available free of charge via the Internet at http://pubs.acs.org.

References and Notes

(1) McKeown, N. B.; Budd, P. M. *Chem. Soc. Rev.* **2006**, *35*, 675–683.
(2) Mackintosh, H. J.; Budd, P. M.; McKeown, N. B. *J. Mater. Chem.* **2008**, *18*, 573–578.
(3) Schmidt, J.; Weber, J.; Epping, J. D.; Antonietti, M.; Thomas, A. *Adv. Mater.* **2009**, *21*, 702–705.
(4) Germain, J.; Svec, F.; Fréchet, J. M. J. *Chem. Mater.* **2008**, *20*, 7069–7076.
(5) Cote, A. P.; Benin, A. I.; Ockwig, N. W.; O'Keeffe, M.; Matzger, A. J.; Yaghi, O. M. *Science* **2005**, *310*, 1166–1170.
(6) El-Kaderi, H. M.; Hunt, J. R.; Mendoza-Cortes, J. L.; Cote, A. P.; Taylor, R. E.; O'Keeffe, M.; Yaghi, O. M. *Science* **2007**, *316*, 268–272.
(7) Han, S. S.; Furukawa, H.; Yaghi, O. M.; Goddard, W. A. *J. Am. Chem. Soc.* **2008**, *130*, 11580–11581.
(8) Wan, S.; Guo, J.; Kim, J.; Ihee, H.; Jiang, D. *Angew. Chem., Int. Ed.* **2008**, *47*, 8826–8830.
(9) Li, Y.; Yang, R. T. *AIChE J.* **2008**, *54*, 269–279.
(10) Kuhn, P.; Antonietti, M.; Thomas, A. *Angew. Chem., Int. Ed.* **2008**, *47*, 3450–3453.
(11) Kuhn, P.; Thomas, A.; Antonietti, M. *Macromolecules* **2009**, *42*, 319–326.
(12) Kuhn, P.; Forget, A. l.; Su, D.; Thomas, A.; Antonietti, M. *J. Am. Chem. Soc.* **2008**, *130*, 13333–13337.
(13) Lee, J. Y.; Wood, C. D.; Bradshaw, D.; Rosseinsky, M. J.; Cooper, A. I. *Chem. Commun.* **2006**, 2670–2672.
(14) Wood, C. D.; Tan, B.; Trewin, A.; Niu, H. J.; Bradshaw, D.; Rosseinsky, M. J.; Khimyak, Y. Z.; Campbell, N. L.; Kirk, R.; Stockel, E.; Cooper, A. I. *Chem. Mater.* **2007**, *19*, 2034–2048.
(15) McKeown, N. B.; Makhseed, S.; Budd, P. M. *Chem. Commun.* **2002**, 2780–2781.
(16) McKeown, N. B.; Hanif, S.; Msayib, K.; Tattershall, C. E.; Budd, P. M. *Chem. Commun.* **2002**, 2782–2783.
(17) Carta, M.; Msayib, K. J.; Budd, P. M.; McKeown, N. B. *Org. Lett.* **2008**, *10*, 2641–2643.
(18) Ghanem, B. S.; McKeown, N. B.; Budd, P. M.; Fritsch, D. *Macromolecules* **2008**, *41*, 1640–1646.
(19) Ghanem, B. S.; Msayib, K. J.; McKeown, N. B.; Harris, K. D. M.; Pan, Z.; Budd, P. M.; Butler, A.; Selbie, J.; Book, D.; Walton, A. *Chem. Commun.* **2007**, 67–69.
(20) Jiang, J. X.; Su, F.; Trewin, A.; Wood, C. D.; Campbell, N. L.; Niu, H.; Dickinson, C.; Ganin, A. Y.; Rosseinsky, M. J.; Khimyak, Y. Z.; Cooper, A. I. *Angew. Chem., Int. Ed.* **2007**, *46*, 8574–8578.
(21) Jiang, J.-X.; Su, F.; Trewin, A.; Wood, C. D.; Niu, H.; Jones, J. T. A.; Khimyak, Y. Z.; Cooper, A. I. *J. Am. Chem. Soc.* **2008**, *130*, 7710–7720.
(22) Stockel, E.; Wu, X. F.; Trewin, A.; Wood, C. D.; Clowes, R.; Campbell, N. L.; Jones, J. T. A.; Khimyak, Y. Z.; Adams, D. J.; Cooper, A. I. *Chem. Commun.* **2009**, 212–214.
(23) Weber, J.; Thomas, A. *J. Am. Chem. Soc.* **2008**, *130*, 6334–6335.
(24) Rose, M.; Bohlmann, W.; Sabo, M.; Kaskel, S. *Chem. Commun.* **2008**, 2462–2464.
(25) Kobayashi, N.; Kijima, M. *J. Mater. Chem.* **2007**, *17*, 4289–4296.
(26) Kobayashi, N.; Kijima, M. *J. Mater. Chem.* **2008**, *18*, 1037–1045.
(27) Schwab, M. G.; Fassbender, B.; Spiess, H. W.; Thomas, A.; Feng, X.; Mullen, K. *J. Am. Chem. Soc.* **2009**, *131*, 7216–7217.
(28) Uribe-Romo, F. J.; Hunt, J. R.; Furukawa, H.; Kloiˆck, C.; O'Keeffe, M.; Yaghi, O. M. *J. Am. Chem. Soc.* **2009**, *131*, 4570–4571.
(29) Jiang, J.-X.; Trewin, A.; Su, F.; Wood, C. D.; Niu, H.; Jones, J. T. A.; Khimyak, Y. Z.; Cooper, A. I. *Macromolecules* **2009**, *42*, 2658–2666.
(30) Lin, X.; Telepeni, I.; Blake, A. J.; Dailly, A.; Brown, C. M.; Simmons, J. M.; Zoppi, M.; Walker, G. S.; Thomas, K. M.; Mays,

T. J.; Hubberstey, P.; Champness, N. R.; Schroder, M. *J. Am. Chem. Soc*. **2009**, *131*, 2159–2171.
(31) Bennett, A. E.; Rienstra, C. M.; Auger, M.; Lakshmi, K. V.; Griffin, R. G. *J. Chem. Phys*. **1995**, *103*, 6951–6958.
(32) Chinchilla, R.; Najera, C. *Chem. Rev*. **2007**, *107*, 874–922.
(33) Littke, A. F.; Fu, G. C. *Angew. Chem., Int. Ed*. **2002**, *41*, 4176–4211.
(34) Jiang, J. X.; Su, F.; Niu, H.; Wood, C. D.; Campbell, N. L.; Khimyak, Y. Z.; Cooper, A. I. *Chem. Commun*. **2008**, 486–488.
(35) Hodgson, D. M.; Selden, D. A.; Dossetter, A. G. *Tetrahedron: Asymmetry* **2003**, *14*, 3841–3849.
(36) Sing, K. S. W.; Everett, D. H.; Haul, R. A. W.; Moscou, L.; Pierotti, R. A.; Rouquerol, J.; Siemieniewska, T. *Pure Appl. Chem*. **1985**, *57*, 603–619.
(37) Sherrington, D. C. *Chem Commun*. **1998**, 2275.
(38) Tavener, S. J.; Clark, J. H.; Gray, G. W.; Heath, P. A.; Macquarrie, D. J. *Chem. Commun*. **1997**, 1147–1148.
(39) Wang, C. *Mater. Lett*. **2008**, *62*, 2377–2380.
(40) Oh, Y. K.; Hong, L. Y.; Asthana, Y.; Kim, D. P. *J. Ind. Eng. Chem*. **2006**, *12*, 911–917.
(41) Kuhn, P.; Kruger, K.; Thomas, A.; Antonietti, M. *Chem. Commun*. **2008**, 5815–5817.
(42) Maffei, A. V.; Budd, P. M.; McKeown, N. B. *Langmuir* **2006**, *22*, 4225–4229.
(43) Wood, C. D.; Tan, B.; Trewin, A.; Su, F.; Rosseinsky, M. J.; Bradshaw, D.; Sun, Y.; Zhou, L.; Cooper, A. I. *Adv. Mater*. **2008**, *20*, 1916–1921.